A STUDY ON THE TREND OF SEA ICE EXTENT IN THE ARCTIC BASED ON THE SATELLITE MICROWAVE OBSERVATIONS

Kohei Cho[1], Ryo Nagashima[2], Kazuhiro Naoki[3],

Tokai University Research & Information Center (TRIC),
2-3-23, Takanawa, Minato-ku, Tokyo, 108-8619, Japan
Email: [1]kohei.cho@tokai-u.jp, [2]ryo.ngsm@fuji.tokai-u.jp, [3]naoki@tokai-u.jp,

KEY WORDS: ice concentration, global warming, AMSR2, cryosphere

ABSTRACT: Due to global warming, sea ice extent in the polar regions, especially in the Arctic, has been dramatically reducing for the last decades. The importance of monitoring the global sea ice extent is increasing. Satellite passive microwave radiometers have been observing the global sea ice distribution since the late 1970s. The sea ice concentration derived from those passive microwave radiometers including AMSR2 on the GCOM-W satellite allows us to monitor the detailed sea ice extent of the whole globe every day. In this study, firstly. the authors have investigated the accuracy of sea ice concentration (IC) estimated from AMSR2 data by comparing it with MODIS data simultaneously observed from the Aqua satellite. Secondly, the authors have compared the sea ice extent images extracted from IC data derived from a time series of satellite passive microwave radiometer observations. The dramatic reduction of sea ice extent in the Arctic was confirmed by composing the minimum and maximum sea ice extent images every two years from 2003 to 2021. Moreover, the result clarified the regional difference in the sea ice extent reduction. Especially, the sea ice extent reduction along the coast of Russia in the summertime was obvious.

1. INTRODUCTION

Global warming is one of the most serious problems we are facing in the 21st Century. The sixth Assessment Report of IPCC (2021) says that human influence is very likely the main driver of the decrease in the Arctic Sea ice area between 1979–1988 and 2010–2019 (decreases of about 40% in September and about 10% in March). These data are mainly derived from the time series of the passive microwave radiometer observations from space starting in 1978 by SMMR on the Nimbus-7 satellite (NASA, 2023). Sea ice concentration is the most typical sea ice parameter which can be calculated from brightness temperatures observed by the microwave radiometers. Sea ice concentration can be defined as the percentage of ice within the unit size of the sea ice area, usually one-pixel size of the brightness temperature data. By multiplying the sea ice concentration of a pixel with a footprint size of a pixel (for example 25km x 25km), one can get the sea ice area within a pixel. Then, by summing the sea ice area of each pixel, one can calculate the total sea ice area of the target area. There are a number of sea ice concentration algorithms including the NASA Team Algorithm (Cavarieli et al., 1984), Bootstrap Algorithm (Comiso, 1995), and ASI Algorithm (2008). It is known that the sea ice concentrations (IC) calculated by the different algorithms are similar, but not the same (Comiso et al., 1997, Alekseeva et al., 2019). Usually, in order to reduce the difference between the IC algorithms, the sea ice extent is calculated by summing all the pixels whose IC is more than 15% (NSIDC, 2008). Figure 1 shows the trend of sea ice extent of the Arctic derived from the time series of passive microwave radiometer observation from space (NPIR, 2023). The reduction trend of the sea ice in the Arctic is clear.

As for AMSR2 onboard GCOM-W satellite, the AMSR Bootstrap Algorithm (Comiso et al., 2009, 2013) is used as the standard algorithm for calculating sea ice concentration from ASMR2 data. Under the contract with JAXA, the authors are evaluating the performance of the algorithm. In this study, first, the authors have evaluated the AMSR2 sea ice concentration accuracy by comparing it with MODIS data under cloudless conditions. And also, evaluated the effect of rejecting the ice concentration area of less than 15% and 10% in sea ice extent extraction. Secondly, the authors have compared the sea ice extent data derived from a time series of satellite passive microwave radiometers, namely AMSR, AMSR-E, AMSR2, and SSM/I. Various

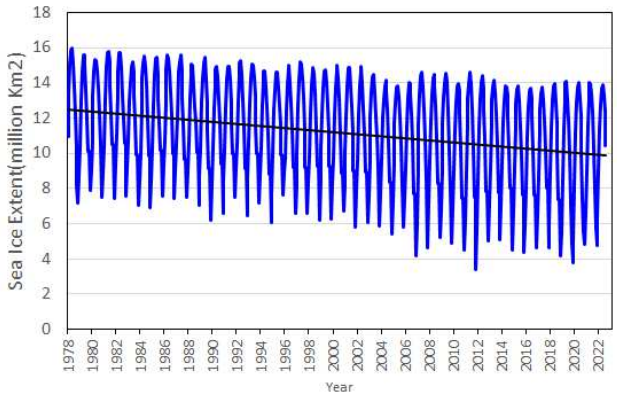

Figure 1. Interannual variability of the Arctic sea ice extent (1978-2023, data source: NASA, JAXA, NPIR)

studies on the trend analysis of sea ice extent and/or IC derived from passive microwave radiometer observations have been performed in the past including Parkinson et al., 1989, Comiso et al., 2008, Cavalieri et al., 2012, and Wang et al., 2020. In this study, the dramatic sea ice extent reduction in the Arctic was confirmed by overlaying the minimum and maximum sea ice extent images of every year from 2003 to 2021 for 19 years. Moreover, the result clarified the regional difference in the sea ice extent reduction in the Arctic.

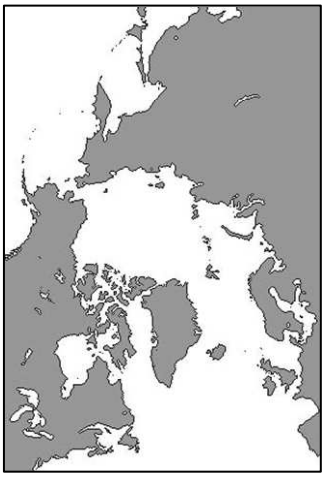

Figure 2. Location map

2. LOCATION MAP

As for the evaluation of the sea ice concentration accuracy of AMSR2, the Sea of Okhotsk was selected. Since the Sea of Okhotsk is the southernmost sea ice zone in the Northern Hemisphere, the sun radiation is more intense than the other sea ice zones of the Northern Hemisphere. Thus, the sea is suitable for evaluating the sea ice concentration accuracy using optical sensor MODIS data. The sea ice extent trend analysis was performed for the Arctic. Figure 2 shows the location map of the analyzed areas.

3. ANALYZED DATA

The AMSR2 sea ice concentration data were analyzed in this study (JAXA, 2012). The sea ice concentration data is one of the AMSR2 standard products produced by JAXA using AMSR-E/AMSR2 Bootstrap Algorithm. One pixel size of the data corresponds to 25km. In order to verify the sea ice concentration calculated from ASMR2 data, optical sensor MODIS band1 and band2 data were used as references. Table 1 shows the specifications of MODIS Band 1 and Band 2. Under the cloud-free condition, detailed distribution of sea ice can be observed from MODIS images. Since both Aqua and GCOM-W satellites are in the same orbit under the framework of NASA's A-Train (NASA, 2012), the constellation of satellites, MODIS onboard Aqua observed the same area four minutes after the observation of AMSR2 onboard GCOM-W. Therefore, MODIS data is one of the most effective validation data for AMSR2 data. In order to utilize the highest spatial resolution of MODIS, we used only Band 1 and 2 which have 250m resolution. Time series of AMSR-E and AMSR2 sea ice concentration data derived by AMSR-E/AMSR2 Bootstrap Algorithm were used for the sea ice extent trend analysis. In order to cover the data loss of 2012, SSM/I sea ice concentration data derived by Bootstrap Algorithm were also used only for 2012 (NSIDC, 2010).

Table 1. Specifications of MODIS (NASA, 2015)

Band	Wavelength	IFOV	Swath
1	0.620-0.670 μm	250 m	2330 km
2	0.841-0.876 μm		

4. METHODOLOGY

4.1 Validation of sea ice concentration and sea ice extent of AMSR2

The authors have been evaluating IC estimated from AMSR2 data using the data of the optical sensor MODIS onboard the Aqua satellite. Since the spatial resolution of MODIS bands 1 and 2 (IFOV=250m) is much higher than the spatial resolution of IC data of AMSR2 (IFOV=25km), detailed sea ice distribution can be observed with MODIS under cloud-free conditions. The procedures of the validation are described in Figure 3. Firstly, MODIS Band 1 data were binarized to discriminate sea ice from open water, and sea ice concentration (the percentage of sea ice in the water) of each pixel size of AMSR2 was calculated using the binarized MODIS data. In this study, the authors have

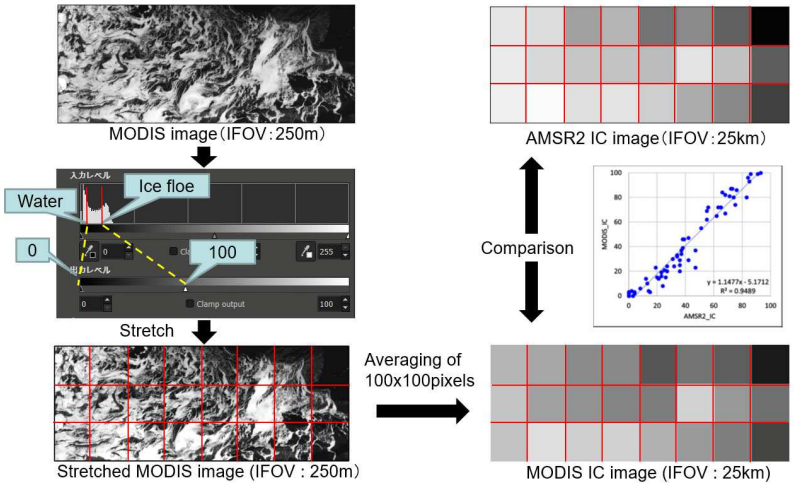

Figure 3. Procedure of validating AMSR2 sea ice concentration using MODIS data.

evaluated how the relationship between IC calculated from MODIS and AMSR2 changes with the threshold level of MODIS data in the Sea of Okhotsk. Then the AMSR2 sea ice concentration of each pixel was compared with the IC calculated from MODIS data. Also, sea ice extent images of rejection levels 15% and 10% were produced and compared with the MODIS image of the same test site observed on the same day.

4.2 Sea ice extent trend analysis of the Northern Hemisphere

In order to evaluate the sea ice extent reduction variability of the Northern Hemisphere, the maximum and minimum sea ice extent images every two years from 2003 to 2021, a total of 10 images for both, were extracted. The 10 maximum extent images were integrated into one image to show the frequency of sea ice existence in the Northern Hemisphere at the time of maximum sea ice extent during the period. The 10 minimum extent images were also integrated into one image in the same manner. The procedure of the image integration is shown in Figure 4. In this case, three times, namely Year N, N+2, and N+4, images were integrated. Figure 4(d) shows the overlay of the sea ice extent images of the three years. Black: no sea ice existed in the three images, dark gray: sea ice existed only once in the three images, middle gray: sea ice existed twice in the three years, white: sea ice existed in all three years. Finally, the frequency difference of sea ice existence was assigned in 10 different colors as shown in Figure 4(e). Originally, the authors started to integrate 20 images of 20 years. However, the composite image with 20 different colors was too busy to see the multi-temporal changes of sea ice extent. As a result, the authors decided to composite a total of 10 images from 2003 to 2021 at one-year intervals.

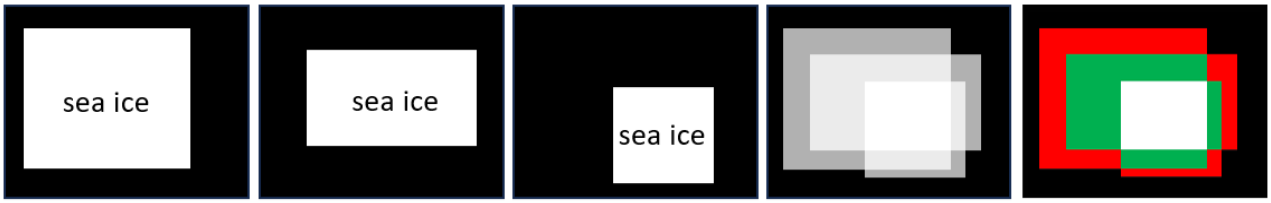

(a)Year N (b)Year N+2 (c) Year N+4 (d) Three years overlay in gray level (e) Three years overlay in color

Figure 4. The concept of composing multiyear sea ice extent images.

5. RESULTS

5.1 Validation of sea ice concentration and sea ice extent of AMSR2

The authors have been validating the accuracy of AMSR2 IC data by comparing it with MODIS IC for years (Cho et al. 2019, 2020). Figures 5 (a) and (b) show a pair of MODIS band 1 and AMSR2 IC images of a part of the Sea of Okhotsk observed on March 29, 2023. Figure 6 shows the scatterplots of AMSR2 IC versus MODIS IC. The RMSE was 5.8%. The authors have validated AMSR2 IC for a total of over 20 scenes. In most cases, the RMSE of AMSR IC against MODIS IC was less than 10%. This result strongly suggests the reliability of AMSR2 IC for calculating sea ice extent.

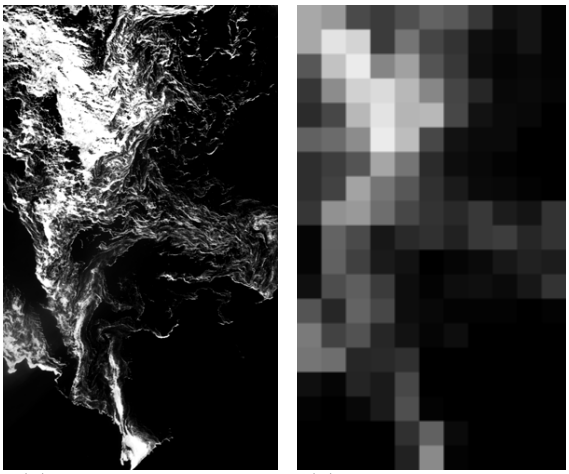

(a) MODIS image (b) AMSR2 IC image

Figure 5. Comparison of MODIS image and AMSR2 IC image (Sea of Okhotsk, Mar. 29, 2023)

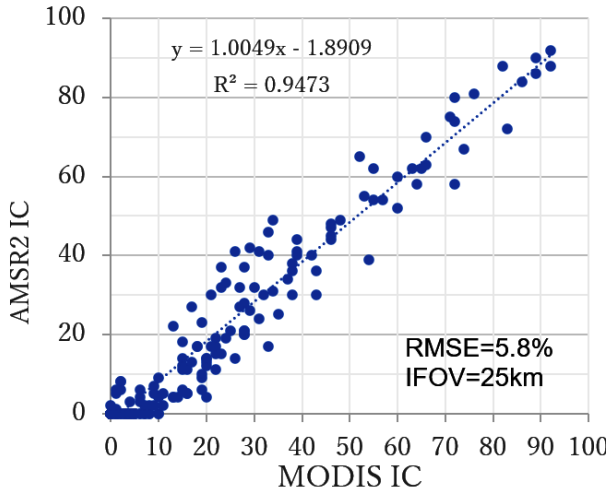

Figure 6. Scatterplots of MODIS IC versus AMSR2 IC (Sea of Okhotsk, Mar. 29, 2023)

Figure 7 shows the sea ice extent images produced from AMSR2 ice concentration data. The sea ice extent of Figure 7(a) was produced by extracting the area where the AMSR2 IC was more than 15%, and the sea ice extent of Figure 7(b) was produced by extracting the area where the AMSR2 IC was more than 15%. MODIS image of the same area is overlayed as references. It is clear that the sea ice extent image of IC > 10% covers more sea ice areas than the sea ice extent image of IC > 15%. However, in this study, the authors used sea ice extent images of IC > 15% to follow the traditional sea ice extent definition of NSIDC.

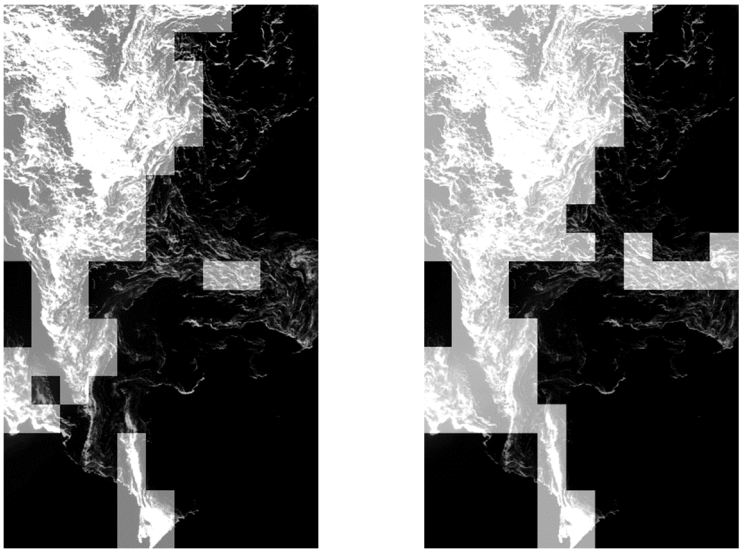

(a) IC >15% (b) IC >10%

Figure 7. AMSRE sea ice extent image comparison with MODIS image overlay (Sea of Okhotsk, Mar. 29, 2023)

5.2 Sea ice extent trend analysis of the Northern Hemisphere

Figure 8 shows the time series of maximum sea ice extent images of AMSR & AMSR2 starting from 2003 to 2021 for every two years, and Figure 9 shows the multiyear frequency image of those. Figure 10 shows the time series of minimum sea ice extent images of AMSR & AMSR2 starting from 2003 to 2021 for every two years, and Figure 11 shows the frequency overlay image of those.

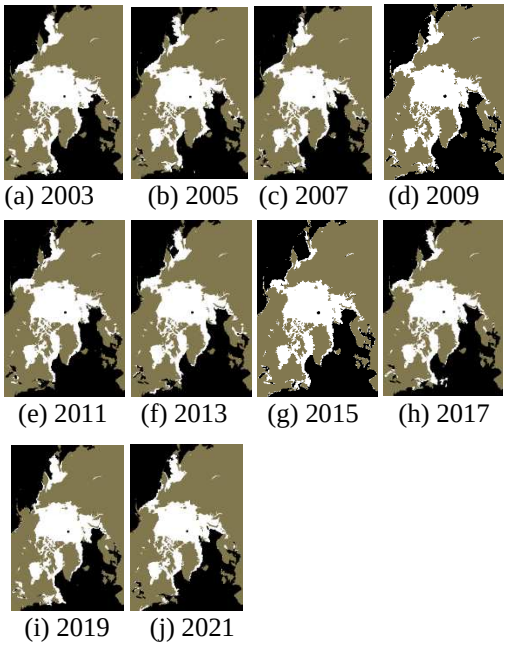

(a) 2003 (b) 2005 (c) 2007 (d) 2009

(e) 2011 (f) 2013 (g) 2015 (h) 2017

(i) 2019 (j) 2021

Figure 8. Time series of maximum sea ice extent from 2003 to 2021 derived from AMSR, AMSR2 and SMM/I data.

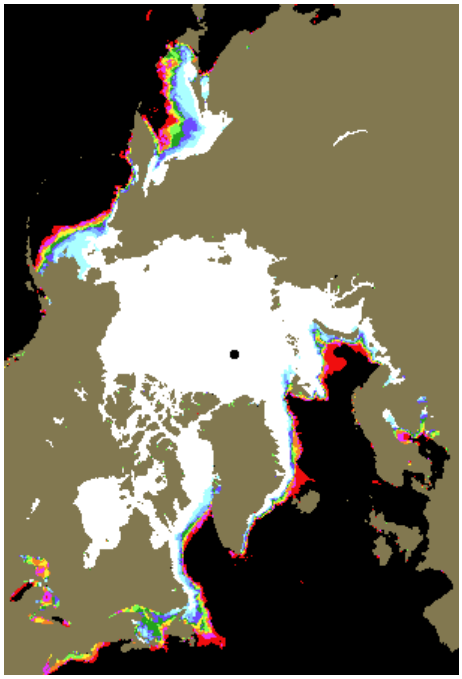

Color	times
	10
	9
	8
	7
	6
	5
	4
	3
	2
	1
	0
	Land

Figure 9. Frequency image of maximum sea ice extent from 2003 to 2021 derived from AMSR, AMSR2 and SMM/I data.

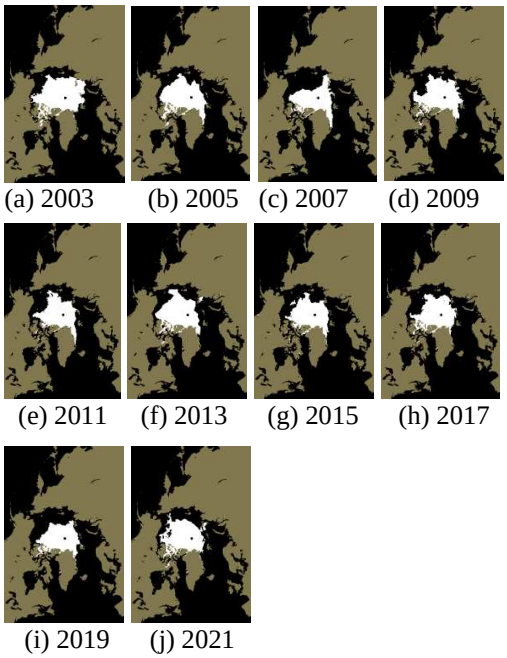

Figure 10. Time series of minimum sea ice extent from 2003 to 2021 derived from AMSR, AMSR2 and SMM/I data.

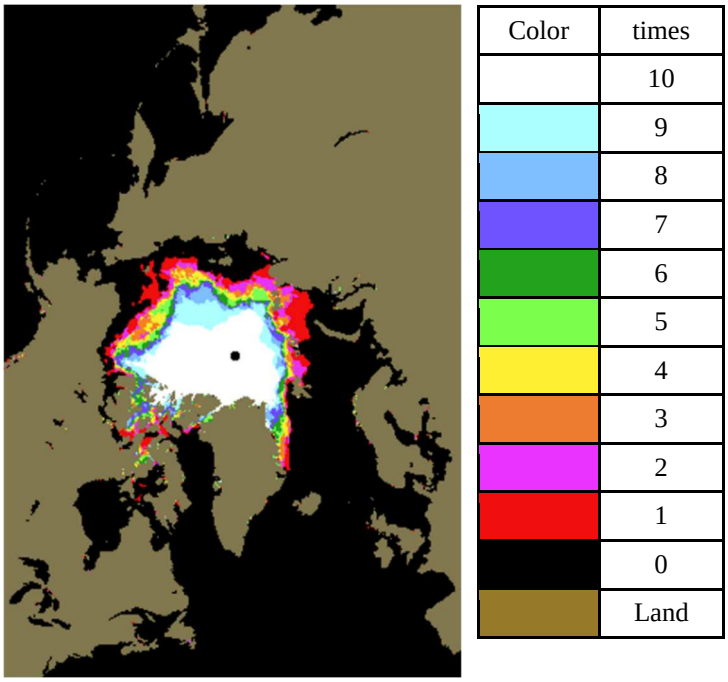

Figure 11. Frequency image of minimum sea ice extent from 2003 to 2021 derived from AMSR, AMSR2 and SMM/I data.

Each color of Figures 8 and 10 corresponds to a certain frequency of the sea ice that existed at that point within the 10 maximum and minimum sea ice extent images of every two years starting from 2003 to 20221. Red means that the sea ice existed only one time at that point within the ten images. White means that the sea ice always existed at that point within the ten images. From Figure 8 we can understand that the multitemporal reduction of the maximum sea ice extent in winter is quite serious in the low latitude sea ice zones namely the Sea of Okhotsk, Bering Sea, Barents Sea, and the Gulf of St. Lawrence. However, the minimum sea ice extent of the high latitude zones including the Arctic Ocean are quite stable at the time of maximum sea ice extent in winter. If we see Figure 10, it is clear that the multitemporal reduction of the minimum sea ice extent in summer on the Russian side of the Arctic Ocean is quite serious. On the other hand, the minimum sea ice extent of the Canadian Archipelago to Greenland is quite stable.

6. CONCLUSION

In this study, firstly. the authors have investigated the accuracy of IC estimated from AMSR2 data by comparing it with MODIS data simultaneously observed from the Aqua satellite. The RMSE of AMSR2 IC was 5.8% for the test site which fulfilled the target accuracy of AMSR2 standard product. Since sea ice extent is calculated from IC data, the accuracy of IC is essential. Secondly, the authors have compared the sea ice extent images extracted from IC data derived from a time series of satellite passive microwave radiometer observations. By composing the minimum and maximum sea ice extent images every two years from 2003 to 2021, the dramatic reduction of sea ice extent in the Arctic was confirmed. Moreover, the result clarified the regional difference in the sea ice extent reduction. Especially, the sea ice extent reduction along the coast of Russia in the summertime was obvious.

Acknowledgments

This study was performed under the sponsorship of the JAXA 3rd Research Announcement on the Earth Observation (EO-RA3). The authors would like to thank all of them for their kind support.

References

IPCC, 2021, “Summary for Policymakers.” in Climate Change 2021: The Physical Science Basis, Contribution of Working Group I to the Fifth Assessment Report.
NASA, 2023, Sea Ice Concentrations from Nimbus-7 SMMR and DMSP SSM/I-SSMIS Passive Microwave Data, Version 1, https://nsidc.org/data/nsidc-0051/versions/1.

Cavalieri, D. J. and P. Gloersen, 1984, Determination of sea ice parameters with the NIMBUS 7 SMMR, J. Geophys. Res., Vol.89, pp.5355-5369.
Comiso, J. C., 1995, SSM/I Sea Ice Concentrations Using the Bootstrap Algorithm", NASA Reference Publication 1380, Maryland, NASA Center for AeroSpace Information.
Spreen G., L. Kaleschke, and G. Heygster, 2008, Sea ice remote sensing using AMSR-E 89 GHz channels, J. Geophys. Res., Vol. 113, C02S03, doi:10.1029/2005JC003384.
Comiso, J. C., D. J. Cavalieri, 1997, C. L. Parkinson, P. Gloersen, Passive microwave algorithms for sea ice concentration: A comparison of two techniques, Remote Sensing of Environment, Vol.60, No.3, pp.357-384.
Alekseeva, T., V. Tikhonov, et. al., 2019, Comparison of Arctic Sea Ice Concentrations from the NASA Team, ASI, and VASIA2 Algorithms with Summer and Winter Ship Data, Remote Sensing, Vol.11(21), No. 2481, https://doi.org/10.3390/rs11212481
NSIDC, 2008, What is the difference between sea ice area and extent?
https://nsidc.org/arcticseaicenews/faq/#area_extent.
NPIR, 2023, VISHOP, https://ads.nipr.ac.jp/vishop/#/monitor
Comiso, J. C., 2009, Enhanced Sea Ice Concentrations and Ice Extent from AMSR-E Data, Journal of the Remote Sensing Society of Japan, Vol.29, No.1, pp.199-215.
Comiso, J. C., K. Cho, 2013, Description of GCOM-W1 AMSR2 Sea Ice Concentration Algorithm, Descriptions of GCOM-W1 AMSR2 Level 1R and Level 2 Algorithms, JAXA, NDX-120015A, (6)1-28, Available online:
http://suzaku.eorc.jaxa.jp/GCOM_W/data/doc/NDX-120015A.pdf
Parkinson C. L., D. J. Cavalieri, 1989, Arctic sea ice 1973-1987: Seasonal, regional, and interannual variability, JGR, Vol. 94, No.C10, pp.14,499-14,523.
Comiso, J. C., F. Nishio, Trends in the sea ice cover using enhanced and comparable AMSR-E, SSM/I, and SMMR data, 2008, JGR, Vol. 113, No.C02S07, https://doi.org/10.1029/2007JC004257.
Cavalieri, D. J. Parkinson C. L., 2012, Arctic sea ice variability and trends, 1979-2010, The Cryosphere, Vol.6, pp.881-889, doi:10.5194/tc-6-881-20112.
Wang, Z., Z. Li, et al., 2020, Spatial and Temporal Variations of Arctic Sea Ice From 2002 to 2017, Earth and Space Science, Vol. 7, Issue 9, doi:10.1029/2020EA001278.
JAXA, 2012, http://suzaku.eorc.jaxa.jp/GCOM_W/w_amsr2/whats_amsr2_j.html.
NASA, 2015, http://modis.gsfc.nasa.gov/about/specifications.php
NASA, 2012, Afternoon Constellation, http://atrain.nasa.gov/
NSIDC, 2023, Sea Ice Trends and Climatologies from SMMR and SSM/I-SSMIS, Version 3,
https://nsidc.org/data/nsidc-0192/versions/3
Cho, K., R. Nagao, K. Naoki, 2019, Validation of AMSR2 sea ice concentration data using MODIS data, Int. Arch. Photogramm. Remote Sens. Spatial Inf. Sci., XLII-2/W13, pp.1741-1746, https://doi.org/10.5194/isprs-archives-XLII-2-W13-1741-2019.
Cho, K., Naoki, K., and Comiso, J. 2020, Detailed Validation of AMSR2 SeaIce Concentration Data using MODIS Data in The Sea of Okhotsk, ISPRS Ann. Photogramm. Remote Sens. Spatial Inf. Sci., V-3-2020, 369–373, https://doi.org/10.5194/isprs-annals-V-3-2020-369-2020.